

# The Porosity of Protective Films on Mild Steel

T. A. KOVACINA

*Physical Chemistry Branch  
Chemistry Division*

December 31, 1968



**NAVAL RESEARCH LABORATORY**  
**Washington, D.C.**

This document has been approved for public release and sale; its distribution is unlimited.

## CONTENTS

Abstract	ii
Problem Status	ii
Authorization	ii
INTRODUCTION	1
EXPERIMENTAL PROCEDURE	2
Sample Preparation	2
Examination of Film for Porous Properties	3
RESULTS	8
Liquid Permeability of Film	8
Uniformity of Film	8
Mean-Pore-Size Determination of Magnetite Films	10
DISCUSSION	13
SUMMARY	14
ACKNOWLEDGMENTS	14
REFERENCES	15

## ABSTRACT

Techniques have been developed for investigation of the porosity of protective films formed in a mild steel-15% NaOH (aqueous) system at 316°C. The apparent porosity and uniformity of the film were determined by hydroxyl ion transport, gas (helium and argon) flow and light transport through the film. Specifically, optical, gas flow, and pore volume per surface area measurements were used to estimate the mean pore size. A comparison of the results from the three methods established an estimated value of 0.1 to 7.0 microns for the mean pore diameter.

## PROBLEM STATUS

This is a final report on this phase of the study; other work is continuing.

## AUTHORIZATION

NRL Problem C06-01  
Project RR 001-05-42-4850

Manuscript submitted August 2, 1968.

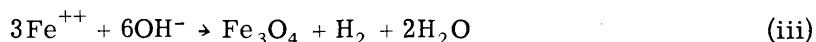
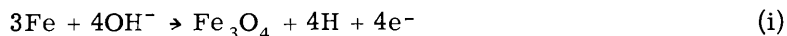
## THE POROSITY OF PROTECTIVE FILMS ON MILD STEEL

### INTRODUCTION

The elucidation of corrosion mechanisms in metal-aqueous systems ideally requires a thorough knowledge of the physical, chemical, and electrochemical properties of the components and their interactions. These interactions are experimentally difficult to identify separately if competitive processes contribute to the overall reaction products. To date, only moderate success has been achieved in the determination of general corrosion mechanisms in the mild steel-aqueous system (high temperature), mainly through evaluation of corrosion rate data and product analysis. The two principal methods used in such studies have been the hydrogen effusion technique of Bloom and Krulfeld (1) and the block specimen-autoclave technique of Potter and Mann (2). The effusion method yields much lower reaction rates and produces apparently homogeneous protective films (3, 4), while the films produced by the autoclave technique are thicker and are characterized by a double-layer structure—a thick outer layer and a relatively thin layer at the metal surface.

A lack of information concerning the physical structure of the films, especially their porosity, has hindered the development of an acceptable explanation of the general corrosion mechanism. Studies (5, 6) of the porosity of the autoclave-grown films of Potter by density and surface area measurements and by electron microscopy have been inconclusive; on the other hand, Castle and Mann (7) suggest on the basis of surface area measurements that the hydrogen-effusion-produced films of Bloom are nonporous. Obviously more definitive studies of the porosity of these oxide films are needed.

The behavior of steel in an aqueous environment at high temperature (8) is characterized by an initial high corrosion rate. As the film thickness increases, corrosion proceeds at a transitory lower rate until finally a much lower steady-state value is approached. The following reactions describe the alternative, or complementary, mechanisms most universally subscribed to:



Reaction i is based on a pore-liquid transport model. The hydroxyl ions in solution gain access to the steel through the porous structure of the film with the formation of magnetite at the steel/oxide interface. Reactions ii and iii suggest a general corrosion mechanism based on solid-state diffusion phenomena. In reaction ii oxide ions from solution diffuse through the film to the steel/oxide interface, where magnetite is again formed. Hydroxyl ion diffusion is similarly envisioned to continue the oxidation of iron at the same site, again according to reaction i. Reaction iii describes the outward diffusion of iron (oxidized at the steel/oxide interface) ions through the film to the oxide/solution interface, where the growth of the magnetite film continues.

The order of magnitude of the pore size would appear to be an important parameter required to determine the feasibility of a general corrosion mechanism based on the

pore-liquid transport model. Access of the corrodent to the underlying metal of the corrosion film by pores of atomic dimensions might reflect corrosion rates comparable to those predicted by a solid-state diffusion mechanism. It is evident that corrosion mechanisms predicted by reaction rate criteria alone might easily be misconstrued. The porosity concept of a general corrosion mechanism has recently been under investigation at NRL. Magnetite films formed in a mild steel—15% NaOH (aqueous) system at 316°C were subjected to various tests conventionally used to examine the porous properties of materials. Methods designed to test the liquid, gas, and visible-light transport properties of stripped, high-integrity films were applied. The treatment of data derived from such experimentation to determine the porosity, uniformity, and mean pore size of the film will be described.

## EXPERIMENTAL PROCEDURE

### Sample Preparation

Capsule and Film Formation - The protective films were formed in cylindrically shaped capsules machined from mild steel bar stock to dimensions of 0.25-in O.D., 0.030-in. wall thickness, and 2.5-in. length. One end of the capsule was machined to a hemispherical shape, and the other end was left open for solution-adding purposes. The capsules were cleaned and heat-treated as follows prior to filling:

1. Polished mechanically.
2. Cleaned ultrasonically by 5-min immersion in an acetone bath, followed by 10 min in a 10/90 acetone-water bath containing 2% of a nonionic detergent (Aquet).
3. Rinsed with water, then with acetone, and stored in a dry atmosphere.
4. Hydrogen annealed at 875°C for 1 hr.
5. Vacuum annealed at 875°C for 1 hr.

The 15% NaOH solution used to load the capsules was prepared from reagent-grade NaOH and distilled water and stored in polyethylene containers. The capsules were half filled (about 1 ml) with the solution to allow for liquid expansion at the temperature of the experiment. No precautions were taken to exclude the ambient room air from the space above the solution. The open end of the capsule was closed by crimping and hermetically sealed by resistance welding. The capsules were then placed in a muffle furnace controlled at 316°C ± 2°C to react for a period of 2 weeks. Films formed under these experimental conditions were about 12 μ thick (8). The reacted capsules were cooled and cut open at the welded end. The liquid solution was withdrawn, and the capsules were repeatedly rinsed with distilled water and organic solvents.

Film-Stripping Procedure - Preferential solution techniques (9) were applied to dissolve the steel backing of the films. The solution of iodine in methanol used does not attack the magnetite film. The outer surface of the capsule was coated with paraffin by immersion in a liquid bath held at a temperature just above the melting point of the wax. The solidified wax was removed only from the closed, rounded end of the capsule to a length approximately 1/4 in. from the bottom. The capsule was then suspended in the iodine-methanol solution in an inert atmosphere (argon), and the steel dissolved from the exposed bottom portion. The stripped surface was repeatedly washed with water-free methanol, until the last traces of iodine disappeared, before removal from the inert

atmosphere. This technique produced a stripped film attached *in situ* to the metal capsule. The combination greatly facilitated the manipulation of the fragile film in the course of the various experimental observations.

Film Integrity - The films were given a crude preliminary screening to establish their physical integrity. The stripped capsules were wetted externally with a detergent soap solution, pressurized inside with helium, and observed for the formation of bubbles to check for extraneous leaks or cracks. The films were observed to exhibit adequate strength to withstand a helium pressure equivalent to at least 5 mm Hg. This was a sufficient pressure for this type of leak test to expose large cracks (invisible to the naked eye) in some films; these were rejected from further consideration. The films were further scrutinized under a microscope at a magnification of at least 300X for similar but smaller defects.

#### Examination of Film for Porous Properties

The following approaches were adopted in probing the stripped film to substantiate or negate its porous structure.

Liquid Transport - To explore in general, the pore concept of the corrosion mechanism suggested by reaction i, it is necessary to deduce whether hydroxyl ions in solution are capable of traversing the film. The investigation of this phenomenon was based on the principle of osmosis. The partially stripped capsule formed in essence a container used for distilled water, which was immersed in a sugar solution in the manner typical of osmotic pressure experiments, using the oxide film as the semipermeable membrane. A diagrammatic view of the assembled apparatus used is shown in Fig. 1. The connection between the capsule and shank of the standard-taper ground-glass joint was made by a close-fitting copper coupling. The lower half of the apparatus, with the exception of the stripped film surface of the capsule, was coated with paraffin to seal all extraneous leaks. The 0.5-mm-bore capillary manometer section fitted with the counterpart taper joint completed the apparatus assembly. A pool of mercury above the combined standard-taper joint assured a positive seal at this juncture.

In a typical experimental run, the lower part of the apparatus containing the iron oxide capsule was carefully filled with distilled water to the top of the standard-taper joint by the use of a hypodermic needle and syringe. The capillary manometer section was next assembled in place by a careful seating of the ground-glass joints. The water level in the measuring capillary was adjusted to a convenient level, and the apparatus was inserted into the sugar solution. The depth of immersion of the apparatus in the solution was about a centimeter from the top of the manometer. The complete assembly was thermostated at 28°C in a water bath. Since the distilled water and solutions used in setting up the apparatus had been stored in the constant-temperature bath, the system was essentially at temperature equilibrium almost immediately on assembly. The water level in the measuring capillary was immediately determined with the aid of a cathetometer, recorded, and compared with the level of solution in the reference capillary. Subsequent measurements were made with time; if any water passed through the film, the volume decrease resulted in a lowering of the water level in the measuring capillary. Osmotic pressures of solutions are conventionally determined by the difference in liquid levels of the respective capillaries, using perfect semipermeable membranes in this type of apparatus. While it is not entirely valid to compare hydroxyl ion (in solution) migration through the film with that of a water molecule, due to electric-charge disparities mainly, it appeared to be a somewhat reasonable approach in consideration of the dipole moment of water.

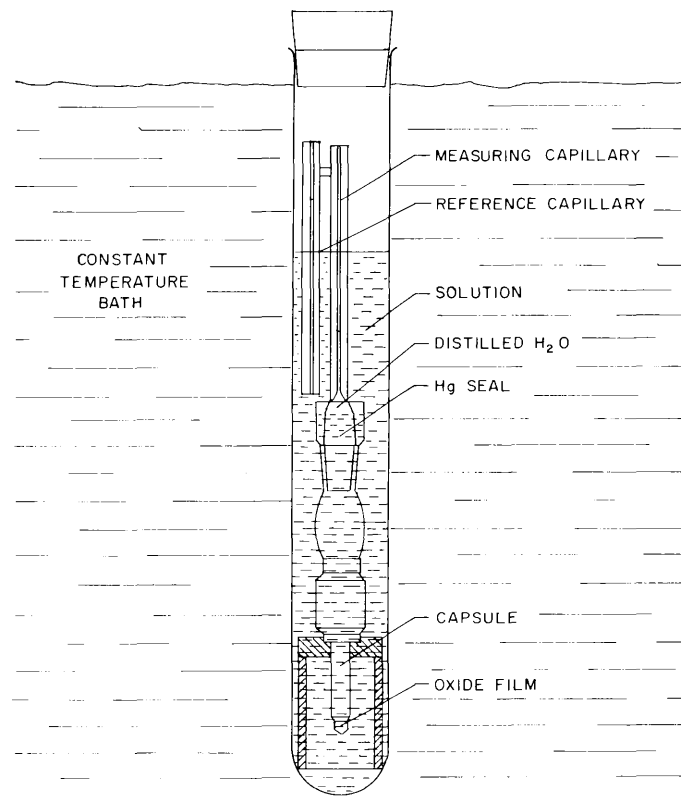


Fig. 1 - Osmotic pressure apparatus

**Gas Transport** - A second approach to this question of the general porosity of the film employed a gas transmission technique. It was designed primarily to detect unusually low flow rates of gas through small orifices (pores). By the variation of the appropriate system parameters, such as the film area and the differential gas pressure across the film, both of which have a controlling effect on the gas flow through the film, additional information concerning the uniformity of the film and mean pore size was obtained.

The experimental apparatus used to investigate the general porosity of the film by this technique is shown in Fig. 2. The same procedure was followed in joining the capsule to the ground-glass joint as previously described for the osmotic pressure apparatus. The gas inside the capsule consisted of an argon (97%)-helium (3%) mixture at a pressure of approximately 2 mm Hg above that of initially pure argon at atmospheric pressure outside of the capsule. Helium was added to the influent argon solely as a tracer for flow. The pressure was regulated by the depth of immersion in the gas bubbler connected in parallel with the gas inlet line to the capsule. Penetration of helium through the iron oxide film was measured with a helium mass spectrometer. The absence of gas flow, indicating no extraneous leak at the tapered joint, was observed under simulated experimental conditions with a sealed glass tube used in place of the test capsule.

The following sequential procedure was pursued in a typical experiment. The flow rates of helium and argon were regulated to give the desired volume-percent composition. With the test capsule removed from the terminal gas inlet line of the apparatus, the gas

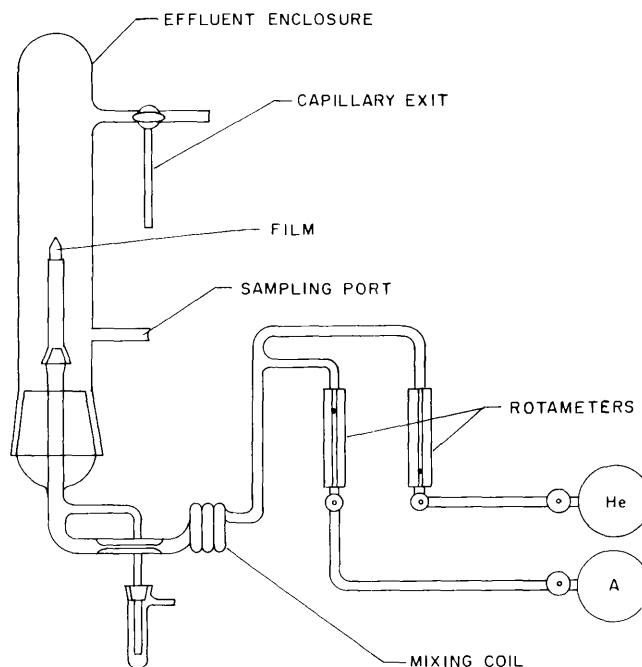


Fig. 2 - Gas transmission apparatus

mixture was flushed through the auxiliary system for about 30 min. This was the minimum time required for homogeneous mixing of the influent gases to occur, as determined by mass spectrometric analysis. This precaution was taken to ensure the constant composition of the gas mixture influent to the test capsule throughout the experiment. The spectrometer probe was permanently connected to the sampling port of the apparatus. An infinitesimal volume of gas flowing through the system was sampled periodically at this juncture until the instrument response to helium remained constant. With the gas mixture flowing through the lines, the effluent gas enclosure of the apparatus was removed and the test capsule placed in position. The removed effluent gas enclosure was repeatedly evacuated and purged with argon and replaced in the system. The effluent gas was periodically sampled for helium as described above to determine gas transport through the film. By comparison of the observed instrument response with a previously prepared calibration curve, the flow of helium through the film could readily be determined.

Film Uniformity - With a slight modification of the experimental conditions described above, the gas transport technique was extended to a study of the uniformity of the film. This was accomplished by measuring the gas flow rate through the film as a function of film area. Due to the uncertainty of reproducing identical film characteristics in different capsules, the area of the stripped film in the same capsule was varied by masking with uncured silicone rubber (General Electric RTV-112). A thin wire rod was dipped into the liquid rubber and removed. The long thin stringer hanging from the end of the wire was directed to the stripped film and used to paint a portion of the surface, care being exercised not to touch the film with the wire. Within a few minutes after application the liquid rubber began to set up and was allowed to cure at room temperature for

at least 24 hr. The flow rate of gas through the exposed film surface of the capsule was measured under otherwise identical experimental conditions as described above. The same procedure was repeated as the film surface was again reduced.

Mean-Pore-Size Determination by Gas Effusion - The concept of the flow rate of gas through porous media (10) is extensively used to obtain very rough estimates of mean pore sizes in materials. The equation for streamline flow (11) has been used to a good advantage for this purpose in certain isolated cases under well-defined conditions. It is based on a capillary pore model of circular cross section and is

$$Q/\Delta P = \frac{\pi E}{\nu} + 1.4 \left( \frac{2\pi n M}{RT} \right)^{1/2} \frac{F}{3} \quad (1)$$

It was derived on the basis of both the geometric parameters of the model and certain applied principles of the kinetic theory of gases. It is a modification of the well-known Poiseuille equation, which states that the mass flow rate of fluid through such a model is proportional to the fourth power of the capillary radius. The second term was added to the Poiseuille equation to correct for enhanced gas flow due to slippage at the capillary wall. In Eq. 1,  $Q$  is the mass flow rate of gas through the capillary;  $\Delta P$  is the pressure differential across the ends;  $\nu$  is the gas kinematic viscosity;  $E$  is  $\pi r^4/\ell$ , where  $r$  is the capillary radius,  $\ell$  is the length, and  $n$  is the total number of such capillaries; and  $F$  is  $\pi r^3/\ell$ . Under streamline flow conditions,  $\Gamma$ , the slip flow constant, has a value near unity (11);  $M$  is the molecular weight of the gas,  $R$  is the gas constant, and  $T$  is the absolute temperature. The equation is immediately recognized as being of the slope-intercept form of a straight line. Thus, if  $Q/\Delta P$  is plotted versus  $1/\nu$ ,  $E$  can readily be calculated from the slope of the line and  $F$  from the  $y$  intercept. The ratio  $E/F$  then is equal to  $r$ , the mean pore radius.

Binary or multicomponent gas mixtures complicate kinetic gas theory calculations on which this method is based by the necessity of corrections for diffusion and segregation effects. In view of these considerations, both the experimental procedure and apparatus design used in the gas transport study of the film were modified slightly as shown in Fig. 3. A different measurement of gas flow through the film became necessary, since the mass spectrometer used previously was designed for helium detection only. Moreover, since the comparative flow rates of different single gases through the same orifice (pore) are used to check the reproducibility of the mean pore size estimate by this technique, it was necessary to incorporate into the system a volumetric flow-measuring device that could be used for any gas. The universal flow meter selected functioned by trapping a soap bubble in the gas stream and timing the gas displacement of a calibrated volume, the soap bubble serving as the marker. A 1.00-ml calibrated volume was used, as low flow rates were anticipated.

A typical run was started by first flushing the assembled apparatus (test capsule removed) with the desired gas for about 20 min to sweep out the ambient room air from the system. In this study either pure helium or argon was used. The test capsule was then placed in position, and the apparatus was reassembled. Before the actual flow measurements through the film were started, the effluent gas from the bubbler was used to flush the system downstream from the capsule for another 30 min. This precaution was taken to ensure the same gas composition on both sides of the film. The gas bubbler was then vented to the atmosphere, and the flow measurements were started by injecting a soap bubble into the gas stream flowing through the film. This was accomplished by squeezing the rubber bulb containing the soap solution and thereby raising the liquid level

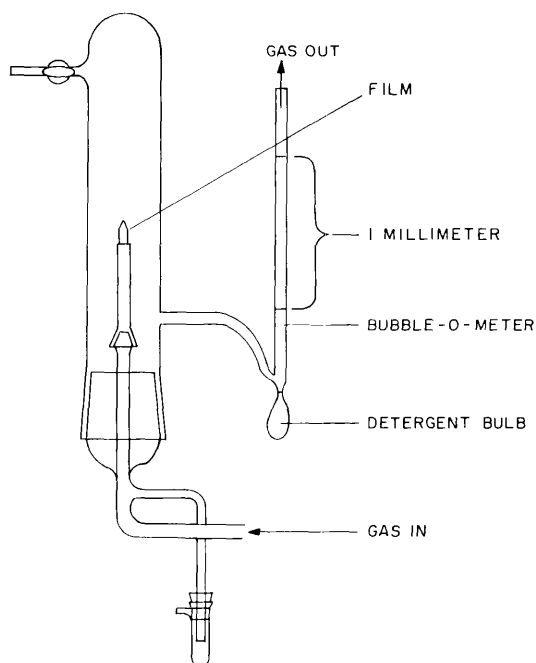


Fig. 3 - Mean pore size-gas flow apparatus

to the gas inlet side arm of the calibrated volume. Flow rate measurements were made as a function of the pressure differential across the oxide film. The gas pressure was regulated as previously described. The maximum pressure differential across the film was equivalent to about 5 mm Hg.

Light Transport - Optical methods present a facile approach to both the qualitative and semiquantitative investigation of the porous properties of materials. The examination of the specimen under the high magnification and resolution of commercially available light microscopic equipment easily permits the investigation of pore sizes in materials down to at least  $0.1 \mu$  in diameter. Photomicrographs of transmitted light patterns of the specimen afford permanent records subject to a variety of analyses which can be related to specimen structure. The intensity of discrete light images (of pores) contrasted against the dark nontransparent background of the specimen enable void fraction estimates and differentiation to be made between pores and cracks. Order of magnitude estimates of the pore size by statistical analysis of the dimensions of the pore images measured microscopically are possible.

The visible-light transmission technique was pursued to supplement the osmotic and gas transport investigations of the film. This approach to the porosity of the film was intended primarily to be qualitative in purpose. However, this technique has been used at NRL (12) with moderate success not only to substantiate the presence of voids in glass-filament-wound composite materials but to estimate their mean diameters (less than  $50 \mu$ ) as well. The specimen (stripped film) to be examined is simply placed under a light microscope and observed for light transmission. The film is impinged with visible light on one side and viewed from the other side under a microscope in a dark field. Light images of the pores in the specimen appear as illuminated spots.

## RESULTS

### Liquid Permeability of Film

The osmotic pressure criterion was adopted primarily to investigate the general liquid permeability characteristics of magnetite films. The film was positioned between a large reservoir (150 ml) of a sucrose solution (40 g/l) and a small reservoir (5 ml) of distilled water (Fig. 1). The data obtained by the procedure previously discussed are in Table 1 and indicate that water indeed passed through the film into the sugar solution. Had there been a large crack or hole in the film, the hydrostatic head of the bulk solution would have counteracted the osmotic pressure effect observed. Evaporative losses of water from the measuring capillary could not have contributed significantly to the observed drop in level.

The experiment was repeated with the same film but with different solutes. This was done for the dual purpose of reproducing the osmotic effect and investigating any sieve effect of the solute molecules by the film. Solutions of raffinose (40 g/l), riboflavin (0.12 g/l), and inulin (0.5 g/l) were used for this purpose. The solute molecular size ranged between 8 and 24 Å in diameter, from sucrose to inulin, respectively. These data, also in Table 1, again demonstrate the liquid permeability of the film. The small osmotic effects typically observed over the long duration of these experiments indicated that back diffusion of solution through the film might have occurred. A quantitative analysis of the liquid in the capsule compartment of the apparatus indicated a solute concentration of 2.5 and 1.5 g/l at the end of the sucrose and raffinose experiments, respectively. Due to the relatively low solubilities of riboflavin and inulin, coupled with the small capacity of the capsule compartment for sampling, only qualitative results were obtained at the end of these experiments, which indicated back diffusion of these larger sized molecules also. On the basis of the low osmotic pressures observed and the lack of a significant solute sieve effect, it was concluded that the pore size of the magnetite films was larger than molecular dimensions.

Comparisons of the observed osmotic pressures with the values expected for perfect semipermeable membranes were obviously of no significance. In addition, the purity of the compounds used in making the solutions and the compatibility of the solutes with the magnetite film (physical and/or chemical adsorption effects) were indeterminate. These phenomena could have contributed to the inconsistencies in the relative osmotic effects observed. The osmotic effect observed with the riboflavin solution was more pronounced than with the sucrose solution, yet the osmotic pressure of the sucrose solution is theoretically greater by a factor of approximately 350.

### Uniformity of Film

As microcracks in the film would likewise reflect an osmotic effect, it is important to differentiate between cracks and pores when postulating corrosion mechanisms. The approach adopted was to investigate the uniformity of the film by measurement of the flow rate of gas through the film as a function of the film area, using the apparatus of Fig. 2. If the films were inherently porous, it appeared reasonable to assume that a uniform pore distribution would exist throughout and that gas flow through the film would be proportional to the film area. Conversely, microcracks of an extraneous nature might be expected to display a more random distribution in the film. In that event, inconsistent flow rates versus film area might be the case.

Table 1  
Osmotic Flow of Water Through a Magnetite Film at 28°C

Sucrose (0.12M)		Raffinose (0.067M)		Riboflavin (0.0003M)		Inulin (0.0005M)	
Elapsed Time (hr)	Pressure Differential (cm H <sub>2</sub> O)	Elapsed Time (hr)	Pressure Differential (cm H <sub>2</sub> O)	Elapsed Time (hr)	Pressure Differential (cm H <sub>2</sub> O)	Elapsed Time (hr)	Pressure Differential (cm H <sub>2</sub> O)
0.0	+0.65*	0.0	-0.75*	0.0	-0.31*	0.0	-1.38*
0.4	+0.60	0.21	-0.91	0.38	-0.33	1.0	1.48
0.9	+0.58	0.45	-0.95	1.50	-0.42	1.7	-1.54
3.1	+0.41	0.78	-0.99	3.05	-0.85	2.4	-1.58
6.4	+0.22	1.90	-1.07	6.30	-1.54	5.0	-1.60
22.0	-1.07	6.40	-1.28	69.80	-4.22	21.0	-1.95
46.4	-2.78	22.30	-2.72	93.70	-4.66	45.0	-2.23
118.9	-2.74	46.50	-3.40	117.86	-4.89	117.5	-2.84
144.8	-2.75	119.5	-8.47	166.30	-5.27	147.2	-2.98
191.7	-2.75	142.6	-8.85	237.78	-7.19	165.1	-3.04
219.6	-2.74	166.3	-9.70	261.76	-8.51	194.5	-3.14
286.2	-2.46			293.10	-10.32	212.5	-3.19
						285.1	-3.49

\*Initial manometer reading relative to reference capillary.

The results of the gas flow-film area experiments are graphically projected as a family of curves in Fig. 4. The initial slopes of the curves were considered to be the most relevant. There are two possible explanations for the reproducible changes in the slopes occurring after approximately 200 min. First, as the helium concentration increased and became more homogeneously mixed with the argon in the enclosed sampling space, the loss of helium by diffusion into the room atmosphere through the capillary exit tube was greatly enhanced. Second, an equilibrium condition was approached as the concentration gradient of helium across the film became greatly reduced, which likewise had the net effect of a reduced flow rate through the film. A comparison of the initial slopes of the family of curves suggests a linear relationship between the gas flow rate and the apparent film area. A more definitive relationship was impossible as the indicated fractions of the original film area through which the flow measurements were made represented approximate values of the visible surface only. However, in view of this consideration, the data generally tend to indicate a film of a fairly uniform nature with respect to the pore distribution.

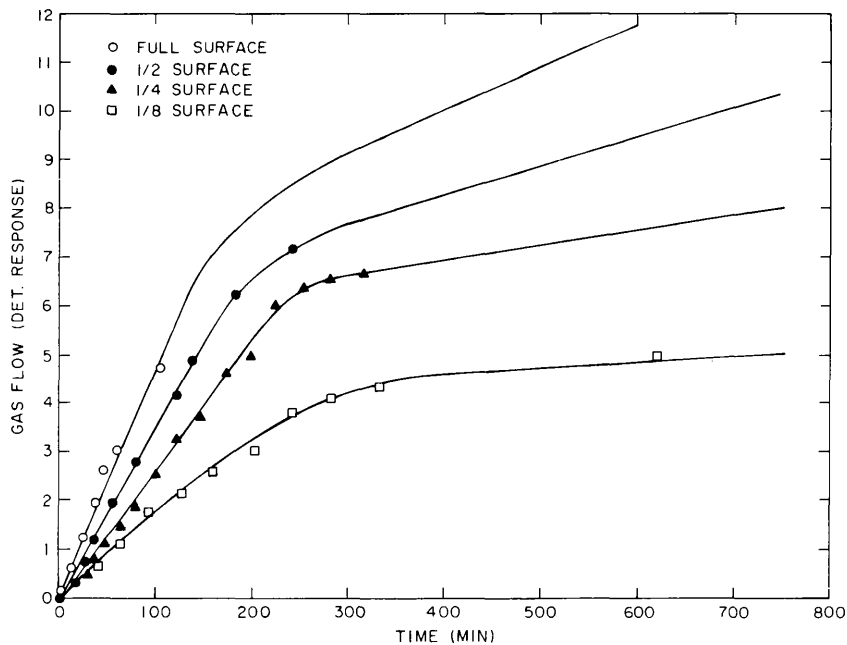


Fig. 4 - Gas flow through magnetite as a function of film surface area

#### Mean-Pore-Size Determination of Magnetite Films

Three different methods of mean-pore-size determination were pursued to obtain the most reasonable estimate of this important quantity possible. It was intended that a comparison of the values obtained by these independent methods would establish order of magnitude agreement, at least.

Gas Flow Method - The application of the streamline flow equation (Eq. 1) was initially used to make a mean-pore-size determination of the film. The flow rates of

both argon and helium through the film were separately measured to determine the reproducibility of the method. Plots of the mass flow rate per unit pressure differential across the film ( $Q/\Delta P$ ) versus the reciprocal kinematic viscosity ( $1/\nu$ ) of the respective gases are shown in Figs. 5 and 6. The data appear to fit the streamline flow equation reasonably well over the limited low-pressure range of the experiments. The slopes of the curves representing the helium and argon data were calculated to be  $4.04 \times 10^{-10}$  and  $2.47 \times 10^{-10}$ , respectively. The corresponding  $y$  intercepts of the curves were found to be  $0.15 \times 10^{-10}$  and  $0.35 \times 10^{-10}$ . Substitution of these values into the appropriate terms of the streamline flow equation enabled the calculation of the desired pore parameter. The comparative results of the helium and argon flow experiments are compiled in Table 2. The derived values of the mean pore diameter appear to be unreasonably large in view of the  $12\text{-}\mu$  thickness of the film. As this method was designed to give a rough estimate of the mean pore size in materials, more reliable approaches were pursued.

**Optical Methods** - A small detached piece of stripped film formed in the usual type capsule was placed under a light microscope and observed for light transmission characteristics by the experimental procedure previously discussed. A photomicrograph of the result is shown in Fig. 7. Due to the extreme curvature of the film specimen, only a portion of the magnified surface was in focus. This surface is represented as the partially discolored (illuminated) area of the photomicrograph. The discrete and irregularly shaped illuminated areas in aggregate formed an apparent replica of the porous surface structure of the film. This replica was compared with those obtained under identical microscopic conditions of standard porous materials to estimate both the mean pore size and void fraction of the film. Commercially available synthetic filter material made to specifications of  $0.1$  and  $0.2 \mu$  in pore diameter and 15% void volume were used as the standard comparators. The basic structure of the standards was of the interconnecting channel type. A comparison of the discrete light patterns of the standards and film specimen revealed a striking similarity in form, which tended to indicate that an interconnecting pore structure was characteristic of the film also. The pore size of the film appeared noticeably smaller than the  $0.2\text{-}\mu$  pore diameter of the larger standard and compared quite favorably with the  $0.1\text{-}\mu$  standard. A comparison of the densities of the discrete, illuminated pore images of the standards and the specimen permitted an estimate of less than 10% for the porosity.

**Void Volume-Surface Area Method** - The void volume-surface area method (10) was derived from a purely mathematical analysis of the geometric parameters of a capillary pore model of circular cross section. The ratio of the specific void volume of a film to its surface area is proportional to  $r/2$ , where  $r$  is the mean pore radius. From the inside dimensions of the capsule in which the film was formed, the film thickness, and porosity function, the void volume of the film can be readily calculated. The porosity of magnetite films formed on mild steel block specimen in 15% NaOH solutions at  $315^\circ\text{C}$  have been determined through direct density measurements by Field, Stanley, Adams, and Holmes (5) to be in the 10 to 15% range. This is in fair agreement with the approximate 10% value estimated by the light microscopy technique of this study. If a porosity value of 10% is assumed, the calculated void volume of the magnetite film formed in the capsule is approximately  $0.0007 \text{ cm}^3$ . The surface area of this same film was determined by the B. E. T. method (13) to be approximately  $500 \text{ cm}^2$ . Four times the ratio ( $0.0007 \text{ cm}^3/500 \text{ cm}^2$ ) gave a calculated value of  $0.056 \mu$  as the mean pore diameter of the magnetite film formed under the experimental conditions of this study.

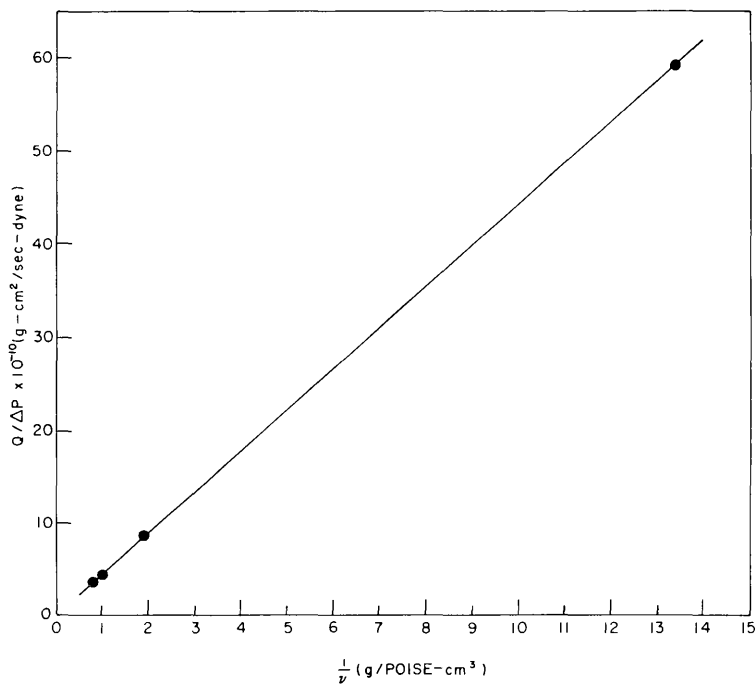


Fig. 5 - Helium flow through magnetite film

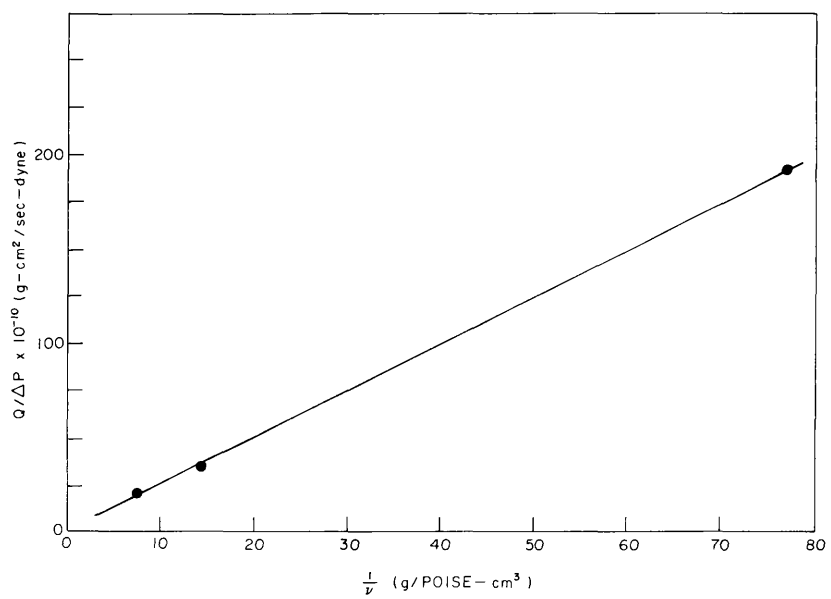


Fig. 6 - Argon flow through magnetite film

Table 2  
Mean Pore Size of Magnetite Films by Helium and Argon Flow Measurements

Gas	E	F	Mean Radius (cm)	Mean Diameter ( $\mu$ )
He	$1.4 \times 10^{-10}$	$0.37 \times 10^{-6}$	$0.37 \times 10^{-3}$	7.3
Ar	$0.8 \times 10^{-10}$	$0.25 \times 10^{-6}$	$0.31 \times 10^{-3}$	6.2

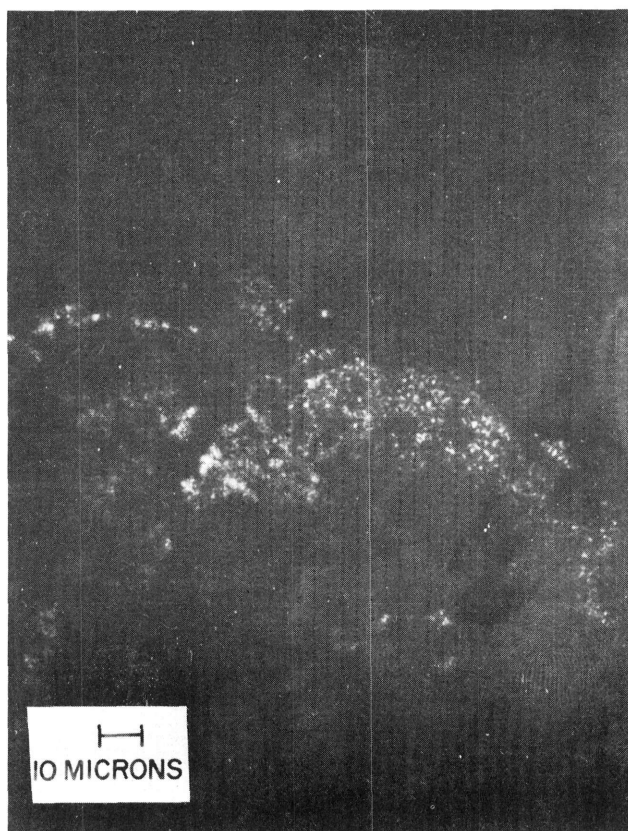
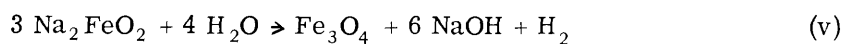
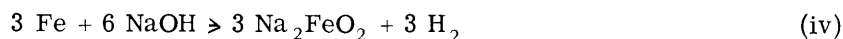


Fig. 7 - Light transmission through magnetite films

## DISCUSSION

Corrosion kinetics observed by numerous researchers in the mild steel-aqueous system at high temperatures reportedly follow various mathematical rate relationships. In general, the corrosion rates observed appear to be too high to justify proposed mechanisms based on solid-state diffusion phenomena of the various system components. Fraser and Bloom (4) proposed a mechanism based on the pore-liquid transport model contingent on a porous structure for the magnetite film. Hydroxyl ions in solution are

envisioned to gain access to the underlying metal of the film by liquid transport through pores, the growth rate of the film being controlled by the liquid phase diffusion of hydroxyl ions to the steel/oxide interface. It might also be controlled by the outward counter diffusion of a soluble iron species such as the  $\text{FeO}_2^{-2}$  ion to the oxide/solution interface as suggested by Castle and Masterson (6). The following reactions illustrate the overall reaction mechanism proposed:



The evidence of the porous nature of magnetite films advanced by the current study lends support to a general corrosion mechanism based on this type of model.

## SUMMARY

The chemical interactions between the various components of a system, such as the metal-corrodent one, can be extremely complex and difficult to define when describing overall reaction mechanisms. Conversely, a knowledge of the physical properties of the reaction products (films) that are direct manifestations of the modes of these interactions can be advantageous in this respect. The effectiveness of magnetite films as corrosion barriers in the mild-steel-aqueous system was investigated from the point of view of their porosity. Qualitative evidence is advanced in support of a general corrosion mechanism based on the pore-liquid transport model.

Techniques were developed for stripping high-integrity magnetite films in a form amenable to various methods of experimental observation. Both liquid and gas permeability criteria were used to substantiate the porous structure of the film. Gas flow rate measurements through the film as a function of film area were used to differentiate between microcracks and pores and to demonstrate the uniform pore distribution. Estimates of the mean pore size by gas flow, optical, and void volume-surface area methods ranged from about 7.0 to 0.1  $\mu$  in diameter, respectively. In view of the better agreement of estimates between the latter two methods (0.1 and 0.06  $\mu$ ) and the relatively thin films (12  $\mu$ ) probed, the submicron range of the mean pore diameter appeared to be more plausible. In any case the pore size is substantially larger than molecular dimensions, permitting ready penetration of water, dissolved salts, and gases through the oxide film.

## ACKNOWLEDGMENTS

The author acknowledges the interest, encouragement, and stimulating discussions of Mr. R. R. Miller and Dr. M. C. Bloom in the course of this study. In addition, the author is greatly indebted to Mr. E. D. Osgood for the preparation of the corrosion capsules, Dr. V. R. Deitz for the B. E. T. measurements, and Messrs. B. E. Walker, Jr., and A. G. Sands for the optical measurements, all of the Chemistry Division of NRL.

## REFERENCES

1. Bloom, M. C. , and Krulfeld, M. , J. Electrochem. Soc. 104:264 (1957)
2. Potter, E. C. , and Mann, G. M. W. , Proceedings of the 1st Int. Congr. Metallic Corrosion, London, 1961, London:Butterworths, pp. 417-426
3. Bloom, M. C. , Proceedings of the 21st Annual Water Conference, Engineers' Society of Western Pennsylvania, 1960
4. Fraser, W. A. , and Bloom, M. C. , Corrosion 18:163 (1962)
5. Field, E. M. , Stanley, R. C. , Adams, A. M. , and Holmes, D. R. , Proceedings of the 2nd Int. Congr. Metallic Corrosion, New York, 1963, Houston, Texas:National Association of Corrosion Engineers, pp. 829-841, 1966
6. Castle, J. E. , and Masterson, H. G. , Corrosion Sci. 6:93 (1966)
7. Castle, J. E. , and Mann, G. M. W. , Corrosion Sci. 6:253 (1966)
8. Bloom, M. C. , Newport, G. N. , and Fraser, W. A. , J. Electrochem. Soc. 111:1343 (1964)
9. Vernon, W. H. J. , Wormwell, F. , and Nurse, T. J. , J. Chem. Soc. (London) 1939:621 (1939)
10. Carmon, P. C. , "Flow of Gases Through Porous Media," New York:Academic Press, 1956
11. Jones, W. M. , and Isaac, P. J. , Trans. Faraday Soc. 55:1947 (1959)
12. Sands, A. G. , Clark, R. C. , and Kohn, E. J. , "An Investigation of Microvoids in Glass-Filament-Wound Structures and the Development of Techniques for Minimizing Their Inclusion," NRL Report 6498, Mar. 31, 1967
13. Brunauer, S. , Emmett, P. H. , and Teller, E. , J. Am. Chem. Soc. 60:309 (1938)

**This page intentionally left blank.**

## DOCUMENT CONTROL DATA - R &amp; D

*(Security classification of title, body of abstract and indexing annotation must be entered when the overall report is classified)*

1. ORIGINATING ACTIVITY (Corporate author) Naval Research Laboratory Washington, D.C. 20390		2a. REPORT SECURITY CLASSIFICATION Unclassified	
		2b. GROUP	
3. REPORT TITLE  THE POROSITY OF PROTECTIVE FILMS ON MILD STEEL			
4. DESCRIPTIVE NOTES (Type of report and inclusive dates) Final report on this phase of the study; work is continuing on other phases.			
5. AUTHOR(S) (First name, middle initial, last name)  T. A. Kovacina			
6. REPORT DATE December 31, 1968		7a. TOTAL NO. OF PAGES 20	7b. NO. OF REFS 13
8a. CONTRACT OR GRANT NO. NRL Problem C06-01		9a. ORIGINATOR'S REPORT NUMBER(S)  NRL Report 6786	
b. PROJECT NO. RR 001-05-41-4850		9b. OTHER REPORT NO(S) (Any other numbers that may be assigned this report)	
c.		d.	
10. DISTRIBUTION STATEMENT  This document has been approved for public release and sale; its distribution is unlimited.			
11. SUPPLEMENTARY NOTES		12. SPONSORING MILITARY ACTIVITY  Department of the Navy (Office of Naval Research, Washington, D.C. 20360	
13. ABSTRACT  Techniques have been developed for investigation of the porosity of protective films formed in a mild steel-15% NaOH (aqueous) system at 316°C. The apparent porosity and uniformity of the film were determined by hydroxyl ion transport, gas (helium and argon) flow and light transport through the film. Specifically, optical, gas flow, and pore volume per surface area measurements were used to estimate the mean pore size. A comparison of the results from the three methods established an estimated value of 0.1 to 7.0 microns for the mean pore diameter.			

14. KEY WORDS	LINK A		LINK B		LINK C	
	ROLE	WT	ROLE	WT	ROLE	WT
Corrosion Porosity Protective films Mild steel Boiler systems						